13.4

High-selective spatially-extended Bragg resonators implementing three-dimensional distributed feedback for powerful free electron lasers

© N.Yu. Peskov [1,2], E.D. Egorova [1], A.S. Sergeev [1], I.M. Tsarkov [1]

[1] Institute of Applied Physics, Russian Academy of Sciences, Nizhny Novgorod, Russia
[2] Budker Institute of Nuclear Physics, Siberian Branch, Russian Academy of Sciences, Novosibirsk, Russia
E-mail: peskov@ipfran.ru

Received September 26, 2022
Revised September 26, 2022
Accepted February 13, 2023.

Novel scheme of Bragg resonators implementing three-dimensional distributed feedback is proposed. The study of their electrodynamic characteristics in the framework of the coupled wave approach has been carried out and high selective properties for the three mode indices have been demonstrated under conditions of substantial oversize. The results of the theoretical analysis are corroborated by the 3D simulations. The prospects of using these resonators in the project of a super-power terahertz-band free electron laser, which is currently being developed at the BINP RAS (Novosibirsk) in collaboration with the IAP RAS (Nizhny Novgorod), are discussed.

Keywords: free-electron lasers, high-power terahertz radiation, Bragg resonators, three-dimensional distributed feedback, mode selection.

DOI: 10.21883/TPL.2023.04.55880.19375

Bragg resonators in the form of waveguide sections with shallow corrugation of side walls are widely used as electrodynamic systems of high-power relativistic masers. These resonators were proposed in [1,2] and implement one-dimensional distributed feedback (DFB). Just as their optical counterparts [3], traditional structures of this type (diagram *1* in Fig. 1, a) provide coupling and mutual scattering of two counter-propagating wave beams: a concurrent one, which interacts synchronously with the electron flow, and a counter one, which establishes the feedback cycle. However, as these resonators grow in size, they lose their selectivity against transverse mode indices (modes with differing transverse structures). At the same time, the construction of higher-power generators based on high-intensity relativistic electron beams and the shift to shorter and shorter wavelengths inevitably lead to enhancement of their oversize factor.

Efficient mode selection in relativistic generators with a transversally extended interaction region may be achieved through the use of the so-called „two-dimensional" Bragg resonators implementing the two-dimensional DFB mechanism [4] (diagram *2* in Fig. 1, a). Resonators of this type feature two-dimensionally periodic corrugation that provides coupling and mutual scattering of four partial waves. Two of these waves propagate along and counter to the electron flow (as in „traditional" resonators), and the other two waves propagate in the transverse direction. Earlier studies have shown that such resonators provide efficient mode selection against the „broad" transverse index (i.e., coordinate x directed along the resonator plates, see Fig. 1) through to a system size of $l_x/\lambda \geqslant 10^2$.

The system may be extended in the second transverse direction (coordinate y directed along the resonator gap) with the use of another type of Bragg structures: the so-called advanced structures, which are specific in that quasi-cutoff waves are introduced into the feedback circuit [5] (diagram *3* in Fig. 1, a). This provides an opportunity to enhance the selectivity of resonators considerably (compared to their „traditional" counterparts) and ensure stable excitation of the operating mode at an interaction region size $a_0/\lambda \sim 20-40$.

The efficiency of resonators of this new type has been verified experimentally in free electron masers/lasers, which have been tested through to the W band at an oversize factor up to 5λ (with the use of advanced Bragg structures [5]) and up to $\sim 50\lambda$ (with two-dimensional structures [4]).

A combination of selection methods in the above-described structure types allows one to enhance the oversize factor in both transverse directions. In the present study, a Bragg resonator implementing the three-dimensional DFB mechanism (Fig. 1, b) is proposed. This resonator is a section of a planar waveguide with corrugation of the following form:

$$a = a_{2\mathrm{D}} \cos(\bar{h}x)\cos(\bar{h}z) + a_{1\mathrm{D}}\left[\cos(\bar{h}z) + \cos(\bar{h}x)\right]. \quad (1)$$

If the Bragg resonance condition

$$\bar{h} \approx h \quad (2)$$

is satisfied, such corrugation provides coupling and mutual scattering of wave flows propagating in three mutually perpendicular directions:

$$\left[\left(A_{+z}e^{-ihz} + A_{-z}e^{ihz} + A_{+x}e^{-ihx} + A_{-x}e^{ihx}\right)\mathbf{E}_A + B\mathbf{E}_B\right]e^{i\omega t}. \quad (3)$$

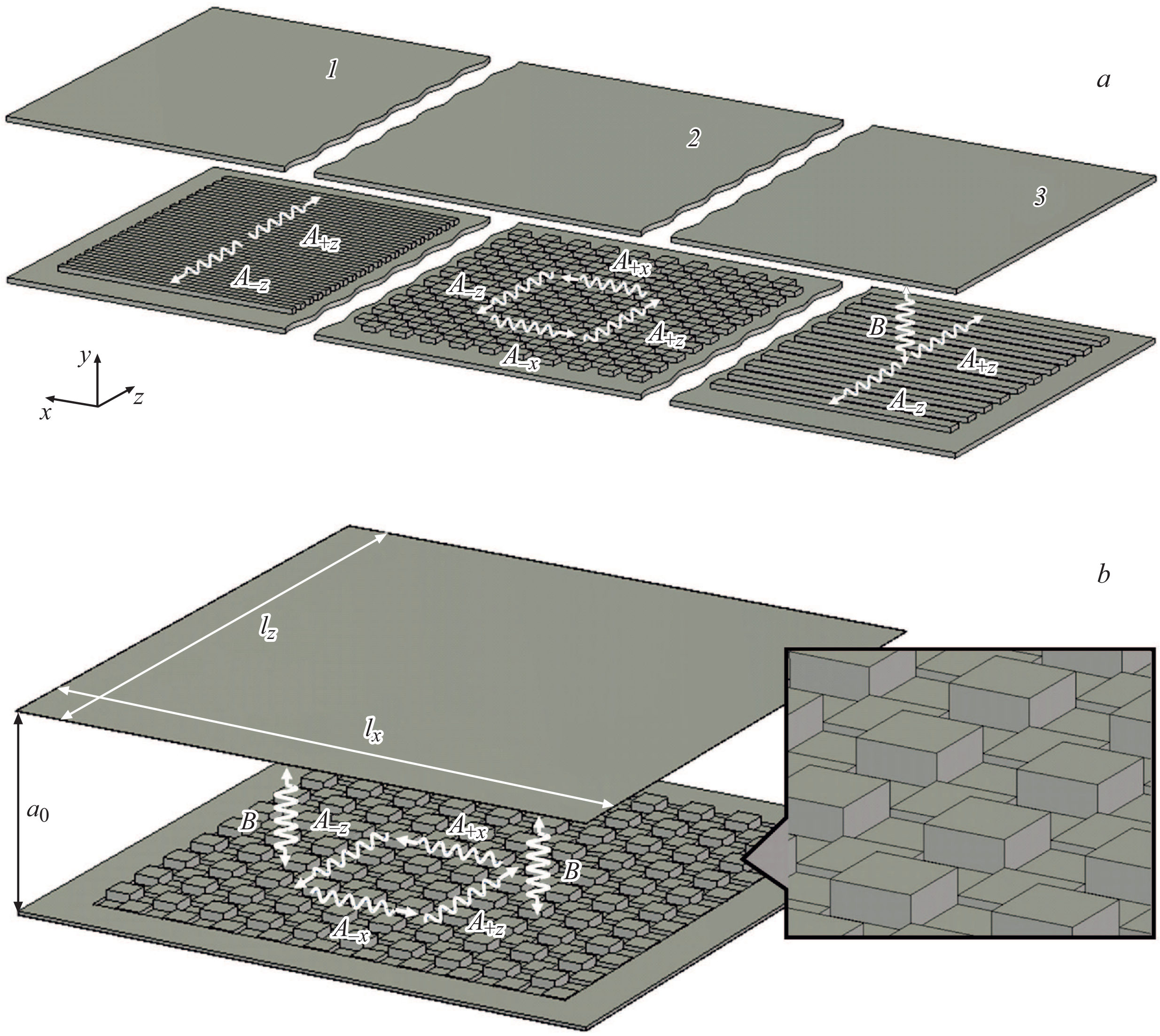

Figure 1. *a* — Known designs of planar Bragg resonators. *1* — „Traditional" Bragg resonator implementing one-dimensional DFB, *2* — Bragg resonator with two-dimensional DFB, and *3* — advanced Bragg resonator with a quasi-cutoff feedback wave. Arrows represent partial wave flows that form a normal wave in each structure type. *b* — Bragg resonator implementing the mechanism of three-dimensional DFB. Geometric sizes are indicated. The corrugation structure of plates in the resonator of this type is shown in the inset.

Specifically, the first term in (1) (as in a two-dimensional Bragg structure [4]) represents mutual scattering of wave flows $A_{\pm z}$ and $A_{\pm x}$ propagating in directions $\pm z$ and $\pm x$, respectively, while the second term (as in advanced Bragg structures [5]) represents the scattering of these waves into quasi-cutoff wave B, which (according to the Brillouin theory) may be interpreted as a standing wave in direction y that is locked between plates forming a planar waveguide. Here, $\bar{h} = 2\pi/d$, d is the corrugation period, a_{1D} and a_{2D} are the amplitudes of the corresponding corrugation „components" (spatial harmonics), $A_{\pm x;\pm z}$ and B are the slowly varying amplitudes of partial waves, and $E_{A,B}$ are functions characterizing the transverse (along axis y) structure of these waves, which matches one of the eigen modes of an unperturbed planar waveguide. Let us assume for simplicity that waves $A_{\pm x;\pm z}$ are of the lowest TEM type. At the same time, wave B is one of the TM_p-waves of a planar waveguide; if the oversize is substantial (i.e., $a_0 \gg \lambda$), it has a high transverse index $p \gg 1$ and, consequently, a multitude of variations along the gap (along coordinate y).

Following the coupled-wave approach, which was detailed in [1], one may characterize the process of mutual scattering of waves (3) off corrugation (1) using the equations for their slowly varying amplitudes $A_{\pm x;\pm z}(x, z)$ and $B(x, z)$ (cf. [4,5]):

$$\partial \hat{A}_{\pm z}/\partial Z \pm i\delta \hat{A}_{\pm z} \mp i\alpha_{2D}\left(\hat{A}_{+x} + \hat{A}_{-x}\right)$$
$$\mp i\alpha_{1D}\hat{B} = 0, \qquad (4a), (4b)$$

$$\partial\hat{A}_{\pm x}/\partial X \pm i\delta\hat{A}_{\pm x} \mp i\alpha_{2D}\big(\hat{A}_{+z} + \hat{A}_{-z}\big)$$
$$\mp i\alpha_{1D}\hat{B} = 0, \qquad (4c), (4d)$$
$$\partial^2\hat{B}/2\partial Z^2 + \partial^2\hat{B}/2\partial X^2 + \big(\delta + \Delta - i\sigma\big)\hat{B}$$
$$- i\alpha_{1D}\big(\hat{A}_{+z} + \hat{A}_{-z} + \hat{A}_{+x} + \hat{A}_{-x}\big) = 0, \qquad (4e)$$

where $(X;Z) = \bar{h}(x;z)$, $\delta = (\omega - \bar{\omega})/\bar{\omega}$ is the detuning between the frequency of partial waves and Bragg resonance frequency $\bar{\omega} = \bar{h}c$, $\Delta = (\bar{\omega} - \omega_c)/\bar{\omega}$ is the detuning between Bragg frequency $\bar{\omega}$ and cutoff frequency ω_c of a quasi-cutoff wave, $\sigma = s/a_0$ is the Ohmic loss parameter, s is the skin layer depth, $(\hat{A}_{\pm x;\pm z};\hat{B}) = (A_{\pm x;\pm z};B)/\sqrt{N_{A;B}}$, and $N_{A;B}$ are norms of the corresponding waves. The coupling coefficients of waves are (cf. [4,5]) $\alpha_{2D} = a_{2D}/4a_0$ and $\alpha_{1D} = a_{1D}/\sqrt{2}a_0$.

Analyzing Eqs. (4), one finds that the considered system under strong coupling ($\alpha L_{x,z} \gg 1$) features a spectrum of high-Q modes, which may be divided into five families. In the geometric optics approximation (i.e., when terms $\sim \partial^2\hat{B}/\partial(X;Z)^2$ in Eq. (4e), which characterize diffraction effects for quasi-cutoff wave B, are neglected), the corresponding solutions for eigenfrequencies $\omega_{n,m} = \bar{\omega}(1 + \mathrm{Re}\delta_{n,m})$ and Q-factors $Q_{n,m} \approx 1/2\mathrm{Im}\delta_{n,m}$ of these modes are given by

$$\delta_{n,m} = \pm(\sqrt{5} \pm 1)\alpha \pm \frac{\pi^2}{4\sqrt{5}\alpha}\left(\frac{n^2}{L_x^2} + \frac{m^2}{L_z^2}\right) + i\left[\frac{\sqrt{5} \pm 1}{2\sqrt{5}}\sigma\right.$$
$$\left. + \frac{\pi^2}{(\sqrt{5} \pm 1)\sqrt{5}\alpha^2}\left(\frac{n^2}{L_x^3} + \frac{m^2}{L_z^3}\right)\right], \qquad (5a), (5b)$$

$$\delta_{n,m} = -2\alpha - \frac{\pi^2}{4\alpha}\left(\frac{n^2}{L_x^2} + \frac{m^2}{L_z^2}\right) + i\left[\sigma + \frac{\pi^2}{2\alpha^2}\left(\frac{n^2}{L_x^3} + \frac{m^2}{L_z^3}\right)\right], \qquad (5c)$$

$$\delta_{n,m} = \frac{\pi^2(n^2 + m^2)}{4\alpha L_x L_z} + i\left[\frac{\pi^2\sigma}{2\alpha^2}\left(\frac{n^2 + m^2}{4L_x L_z} + \frac{m^2 n^2}{n^2 L_z^2 + m^2 L_x^2}\right)\right.$$
$$\left. + \frac{\pi^2(n^2 + m^2)^2}{4\alpha^2(n^2 L_z^2 + m^2 L_x^2)}\left(\frac{1}{L_x} + \frac{1}{L_z}\right)\right], \qquad (5d)$$

$$\delta_{n,m} = -\Delta + i\sigma, \qquad (5e)$$

where $n = 0, \pm1, \pm2\ldots$ is the transverse (along axis x) mode index, and $m = 0, \pm1, \pm2\ldots$ is the longitudinal (along axis z) mode index. The eigenmode spectrum of the resonator was determined under the assumption of zero external electromagnetic fluxes and perfect matching for partial waves in emission from the resonator. For simplicity, Eqs. (5a)–(5e) were derived under the assumption that the coupling coefficients of waves remain the same in different feedback cycles: $\alpha_{2D} \approx \alpha_{1D} \equiv \alpha$; it was also assumed that $\Delta \ll \alpha$.

The spectrum of resonator modes determined within the geometric optics approximation of the coupled-wave approach at $\alpha L_x = \alpha L_z = 3$ is presented in Fig. 2 (dimensions are the same as those of a resonator examined in a subsequent numerical simulation). The frequencies

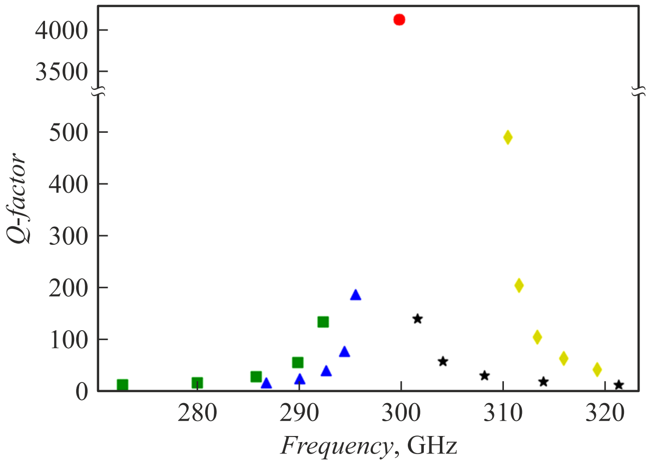

Figure 2. Mode spectrum of the „three-dimensional" planar Bragg resonator within the geometric optics approximation. Diamonds, triangles, squares, and asterisks correspond to mode families *1* (solutions (5a)), *2* (5b), *3* (5c), and *4* (5d). The filled circle denotes the eigenmode from family *5* (degenerate family specified by solutions (5e)). Its frequency and Q-factor were determined in CST simulations.

of modes are located in the vicinity of $\delta \approx (\sqrt{5} + 1)\alpha$ and $\delta \approx -(\sqrt{5} - 1)\alpha$ (families *1* and *2* specified by (5a) and (5b)), $\delta \approx -2\alpha$ (family *3*, (5c)), $\delta \approx 0$ (family *4*, (5d)), and $\delta \approx -\Delta$ (family *5*, (5e)). According to our analysis, the fundamental mode with the highest Q-factor belongs to family *5*. However, modes of this family are degenerate within the considered approximation in both frequency $\mathrm{Re}\delta_{n,m} \approx -\Delta$ (that matches the cutoff frequency of quasi-cutoff wave B, which forms the feedback circuit; i.e., $\omega_{n,m} \approx \omega_c$) and Q-factor, which is limited by Ohmic losses only: $Q_{n,m} = Q_{Ohm} \approx 1/2\sigma$. This degeneracy is the result of straightening of dispersion curves in the case when diffraction effects are neglected in Eq. (4e).

Simulations with CST Microwave Studio were performed to verify the results of theoretical analysis obtained within the coupled-wave approach. The Bragg resonator implementing the three-dimensional DFB mechanism was designed to operate in a frequency band around 0.3 THz and had the following parameters: $l_x = l_z = 50$ mm (i.e., $\sim 50\lambda$), $a_0 = 5$ mm ($\sim 5\lambda$), $d = 1$ mm, $a_{1D} = 0.05$ mm, and $a_{2D} = 0.14$ mm (thus, $\alpha_{2D} \approx \alpha_{1D}$). Periodic meander-type functions (see the inset of Fig. 1, *b*) were used to approximate harmonic functions (1). The structure was excited by a short electromagnetic pulse of a dipole located within it.

The results of modeling of spatiotemporal dynamics of the high-frequency (HF) field in the resonator are shown in Fig. 3, *a*, which presents the HF field spectra at the initial ($1 \leqslant t \leqslant 6$ ns) and end ($10 \leqslant t \leqslant 15$ ns) stages of evolution. These results suggest that a large number of eigenmodes of the structure belonging to different families are excited at the initial stage. Their frequencies agree closely with solutions (5a)–(5e). The decay and de-excitation of waves

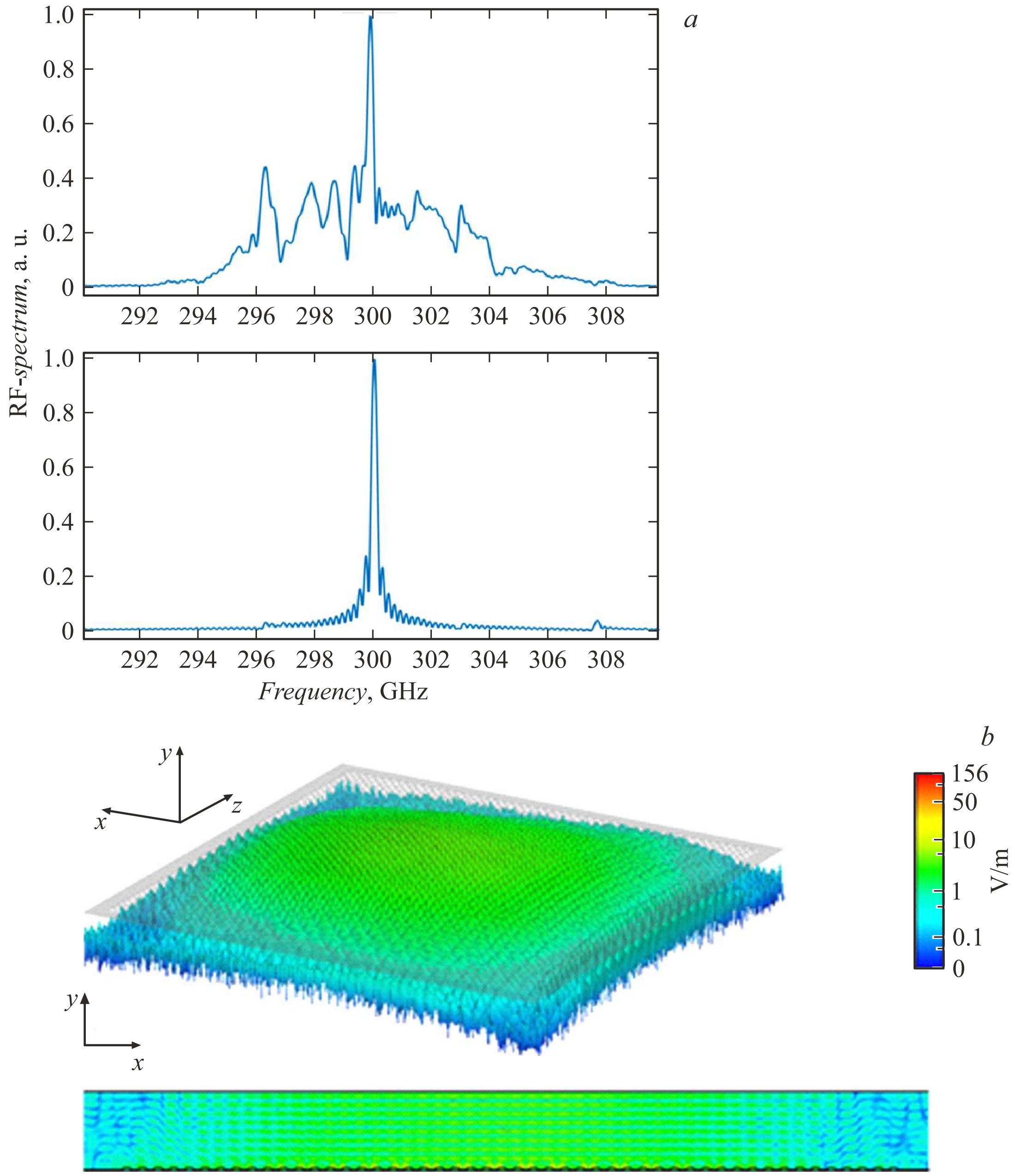

Figure 3. Results of CST modeling of the „three-dimensional" Bragg resonator in the sub-terahertz frequency range. *a* — HF field spectra at the initial (upper fragment) and final (lower fragment) stages; *b* — spatial structure of the HF field in the resonator at the final stage of evolution.

then occur over times that are inversely proportional to their Q-factors. Consequently, the fundamental mode with the highest Q-factor, which is located at the center of the band of Bragg scattering at the exact resonance frequency specified by relation (2), is singled out at the final stage (the modeled resonator parameters corresponded to $\Delta = 0$; i.e., $\bar{\omega} \approx \omega_c$). The HF field decay factor may be used to estimate the Q-factor of this mode: $Q \sim 4500$. The structure of the HF field in the resonator at the final stage of evolution (see Fig. 3, *b*) verifies that a normal wave, which is shaped by the specified combination of partial wave flows in the form of four travelling TEM waves and a quasi-cutoff TM_{10} wave, is established in the resonator.

Thus, the results of theoretical analysis and computer modeling reveal fine selectivity of the proposed spatially-extended Bragg resonators that implement the three-dimensional DFB mechanism. These resonators have high potential to be used as electrodynamic systems of free electron lasers and may support stable single-mode lasing under the conditions of substantial oversize in sub-terahertz and terahertz ranges. Free electron lasers operating in these ranges at sub-gigawatt and gigawatt power levels with a pulse energy content of $\sim 10-100$ J, which exceeds the one typical of known world-class laser systems of this kind, are currently being constructed based on a linear induction accelerator [6] at the BINP RAS (Novosibirsk) in collaboration with the IAP RAS (Nizhny Novgorod).

Funding

This study was supported in part by the Russian Science Foundation (grant No. 19-12-00212).

Conflict of interest

The authors declare that they have no conflict of interest.

References

[1] N.F. Kovalev, I.M. Orlova, M.I. Petelin, Radiophys. Quantum Electron., **11** (5), 449 (1968). DOI: 10.1007/BF01034380.
[2] V.L. Bratman, N.S. Ginzburg, G.G. Denisov, Sov. Tech. Phys. Lett., **7**, 565 (1981)..
[3] A. Yariv, *Quantum electronics* (John Wiley and Sons, Inc., N.Y., 1975).
[4] A.V. Arzhannikov, N.S. Ginzburg, P.V. Kalinin, S.A. Kuznetsov, A.M. Malkin, N.Yu. Peskov, A.S. Sergeev, S.L.Sinitsky, V.D. Stepanov, M. Thumm, V.Yu. Zaslavsky, Phys. Rev. Lett., **117** (11), 114801 (2016). DOI: 10.1103/PhysRevLett.117.114801
[5] N.Yu. Peskov, N.S. Ginzburg, I.I. Golubev, S.M. Golubykh, A.K. Kaminsky, A.P. Kozlov, A.M. Malkin, S.N. Sedykh, A.S. Sergeev, A.I. Sidorov, V.Yu. Zaslavsky, Appl. Phys. Lett., **116** (21), 213505 (2020). DOI: 10.1063/5.0006047
[6] D.A. Nikiforov, A.V. Petrenko, S.L. Sinitsky, P.A. Bak, D.I. Skovorodin, P.V. Logachev, K.I. Zhivankov, E.S. Sandalov, O.I. Meshkov, A.V. Ivanov, V.V. Fedorov, A.A. Starostenko, O.A. Pavlov, G.I. Kuznetsov, A.A. Krylov, D.A. Starostenko, O.A. Nikitin, A.R. Akhmetov, J. Instrum., **16**, P11024 (2021). DOI: 10.1088/1748-0221/16/11/P11024